

PSFC/JA-06-8

## **A monoenergetic proton backlighter for measuring E and B fields and for radiographing implosions**

**C. K. Li,<sup>1</sup> F. H. Seguin,<sup>1</sup> J. A. Frenje,<sup>1</sup> R. Rygg,<sup>1</sup> R. D.  
Petrasso<sup>1</sup>, R. P. J. Town,<sup>2</sup> P. A. Amendt,<sup>2</sup> S. P. Hatchett,<sup>2</sup>  
O. L. Landen,<sup>2</sup> A. Mackinnon,<sup>2</sup> P. K. Patel,<sup>2</sup>  
V. Smalyak,<sup>3</sup> J. P. Knauer,<sup>3</sup> T. C. Sangster,<sup>3</sup> C. Stoeckl<sup>3</sup>**

**10 May 2006**

<sup>1</sup> **Plasma Science and Fusion Center, Massachusetts Institute  
of Technology, Cambridge, Massachusetts 02139**

<sup>2</sup> **Lawrence Livermore national Laboratory,  
Livermore, California 94550**

<sup>3</sup> **Laboratory for Laser Energetics, University of Rochester,  
Rochester, New York 14623**

The work described here was performed in part at the LLE National Laser User's Facility (NLUF), and was supported in part by US DOE (Grant No. DE-FG03-03SF22691), LLNL (subcontract Grant No. B504974), and LLE (subcontract Grant No. 412160-001G).

Submitted to *Review of Scientific Instruments* for Invited Talk at 16<sup>th</sup> High-Temperature Plasma Diagnostic meeting, May 8-11, 2006 Williamsburg VA.

# A monoenergetic proton backlighter for measuring E and B fields and for radiographing implosions and HED plasmas

C. K. Li, F. H. Séguin, J. A. Frenje, J. R. Rygg, R. D. Petrasso

*Plasma Science and Fusion Center, Massachusetts Institute of Technology, Cambridge, Massachusetts 02139*

R. P. J. Town, P. A. Amendt, S.P. Hatchett, O. L. Landen, A. J. Mackinnon,  
P. K. Patel

*Lawrence Livermore national Laboratory, Livermore, California 94550*

V. A. Smalyuk, J. P. Knauer, T. C. Sangster, C. Stoeckl

*Laboratory for Laser Energetics, University of Rochester, Rochester, New York 14623*

## Abstract

A novel monoenergetic proton backlighter source and matched imaging detector have been utilized on the OMEGA laser system to study electric (E) and magnetic (B) fields generated by laser-plasma interactions, and will be utilized in the future to radiograph implosions and high-energy density (HED) plasmas. The backlighter consists of an imploding glass micro-balloon with  $D^3He$  fuel, producing 14.7-MeV  $D^3He$  protons and 3-MeV DD protons that are then passed through a mesh that divides the protons into beamlets. For quantitative study of E+B field structure, monoenergetic protons have several unique advantages compared to the broad energy spectrum used in previous experiments. Recent experiments have been performed with a single laser beam (intensity  $\sim 10^{14}$  W/cm<sup>2</sup>) interacting with a CH foil, and B fields of  $\sim 0.5$  MG and E fields of  $\sim 2 \times 10^8$  V/m have been measured using proton deflectometry. LASNEX simulations are being used to interpret these experiments. Additional information will also be presented on the application of this technique to measuring E and B fields associated with hohlraums and directly driven implosions, to radiographically mapping the areal density ( $\rho R$ ) distribution in imploded capsules, and to radiographing HED plasmas.

## I. INTRODUCTION

Probing plasma conditions with radiography, utilizing an external backlighter source of radiation or particles, provides important diagnostic information that is different from information obtained by measuring plasma self emissions. In inertial confinement fusion (ICF),<sup>1,2</sup> for example, x-ray backlighting has been widely used to diagnose plasma conditions associated with the variations of density and temperature, such as those due to hydrodynamic instabilities and shock wave propagation, etc.<sup>3-5</sup> Proton radiography has been proposed as another important diagnostic method for probing plasmas, because it is sensitive to both density and electromagnetic fields. Fields can be measured through the deflections they induce in proton trajectories,<sup>6-8</sup> and recent work by Mackinnon *et al.*<sup>6</sup> demonstrated that high-resolution images containing deflection information could be obtained, although no direct connections were made between images and fields. In their experiment, backlighter protons were generated by irradiating a solid tungsten target with a high-intensity petawatt laser beam (duration 300 fs with intensity  $1 \times 10^{19}$  W/cm<sup>2</sup>); the result was a large proton flux and a continuous energy spectrum up to  $\sim 50$  MeV. These

protons were passed through a mesh and used to image a plasma generated by a single laser beam (300 ps) on a 120- $\mu\text{m}$  Cu wire. More recently, work by Romagnani, *et al.*,<sup>7</sup> utilized side-on proton radiography to study the E field generated by a high-intensity ( $\sim 10^{18}$  W/cm<sup>2</sup>), short-pulse ( $\sim 1.5$  ps) laser driving an Au foil. In their experiments, the probing proton flux had a continuous energy spectrum and was generated from a 10- $\mu\text{m}$  Au foil irradiated by a laser pulse  $\sim 300$  fs at the intensity  $\sim 2 \times 10^{19}$  W/cm<sup>2</sup>.

We have recently taken a different approach, backlighting laser-plasma interactions with multiple monoenergetic protons<sup>9</sup>. Experiments have demonstrated that such an approach has distinct advantages over radiography with broad-band proton sources (such as intense-laser-induced sources). With our sophisticated CR-39 detector system,<sup>10,11</sup> high-resolution, time-gated, single-energy proton radiography images have been obtained and allow us to make precise, unambiguous connections between the experimental data and computer simulations. The monoenergetic charged particles of particular interest are 14.7-MeV D<sup>3</sup>He protons and 3-MeV DD protons that are fusion products of the nuclear reactions



and



that occur in implosions of D<sup>3</sup>He-filled ICF capsules (see Fig. 1).

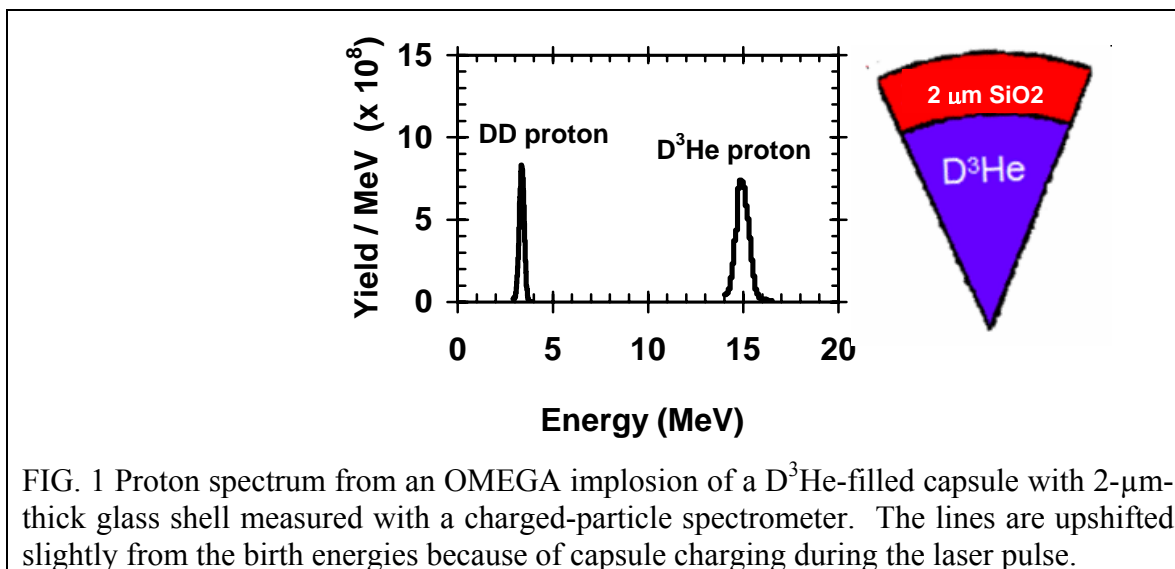


FIG. 1 Proton spectrum from an OMEGA implosion of a D<sup>3</sup>He-filled capsule with 2- $\mu\text{m}$ -thick glass shell measured with a charged-particle spectrometer. The lines are upshifted slightly from the birth energies because of capsule charging during the laser pulse.

These protons have been used extensively to study many aspects of the imploded capsules themselves, including areal density ( $\rho R$ ) and  $\rho R$  asymmetries, spatial distributions of nuclear burn, shock yields, and implosion dynamics.<sup>12-19</sup> The extensive experience we have had during the last decade studying proton generation characteristics and developing proton detection technology for spectrometry and imaging have allowed us to utilize our unique technology for backlit imaging with monoenergetic protons.

This paper is organized as follows: Section II discusses the backlighter characteristics and our detection system. We present the preliminary experimental

measurements of recent E/B field measurements in Section III. A number of important physics problems we are planning to address using this technology are discussed in Section IV, and our results are summarized in Section V.

## II. A MONOENERGETIC PROTON BACKLIGHTER WITH MATCHED DETECTION SYSTEM

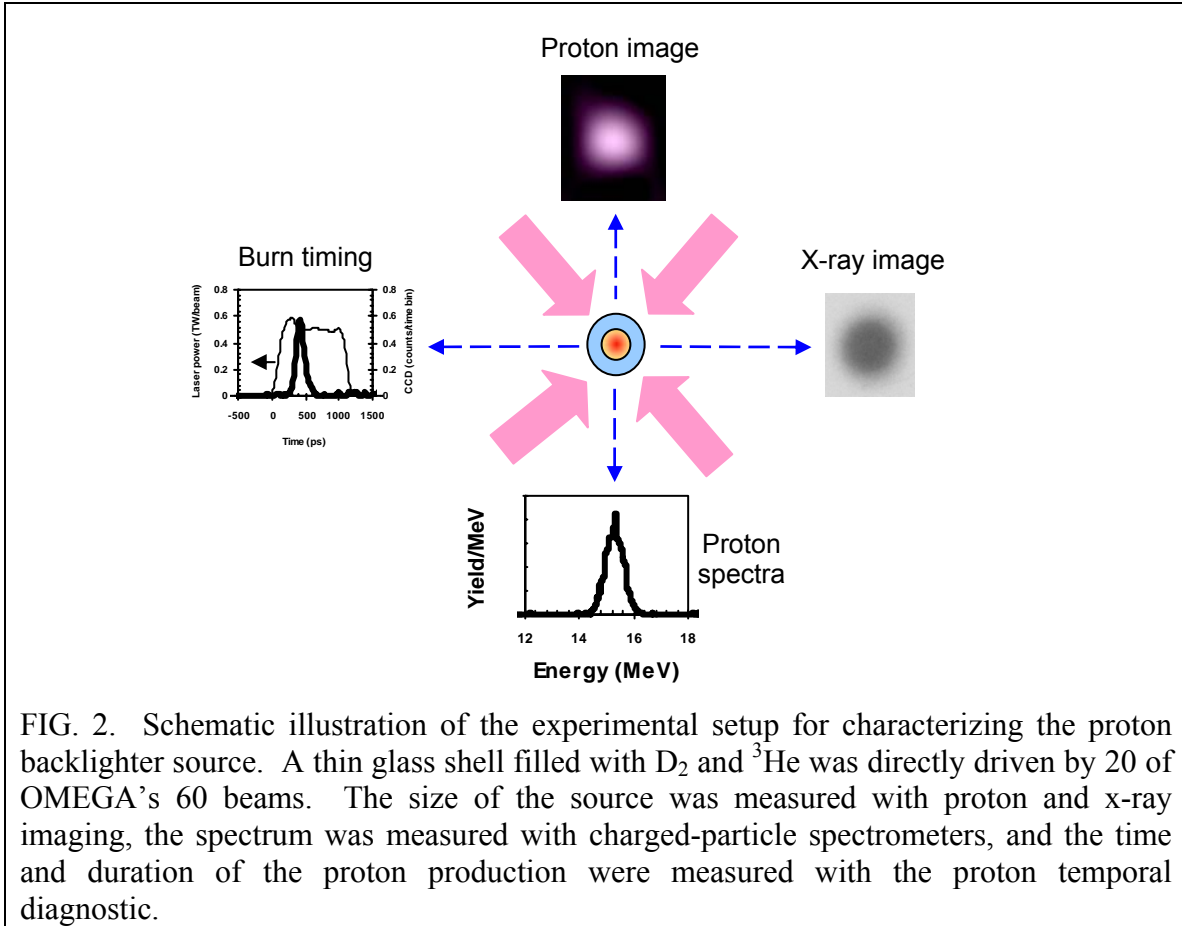
### A. Characteristics of proton backlighters

The backlighter is formed by an exploding-pusher implosion with a  $D^3He$ -filled, glass-shell capsule driven by 20 of the 60 OMEGA laser beams.<sup>20</sup> The implosion laser delivered  $\sim 10$  kJ in a 1-ns square pulse. The capsule diameter used was smaller than a standard OMEGA capsule, at about  $420 \mu\text{m}$ , in order to minimize the burn radius and thus optimize the spatial resolution of the radiograph. No phase plates or SSD were applied. Fig. 2 schematically illustrates the experimental setup for characterizing the proton backlighter source. A comprehensive set of diagnostics was used to characterize the implosions. Proton and x-ray images indicated that the source of the protons was nearly spherical, with a radial emission profile approximately Gaussian with  $1/e$  radius  $\sim 27 \mu\text{m}$ .<sup>9</sup> Proton spectrometers determined that  $10^7$ - $10^9$   $D^3He$  and DD protons were emitted with mean energies 15-15.3 MeV and 3.2-3.5 MeV, respectively; these energies are several hundreds keV higher than the corresponding proton birth energies because of capsule charging, a phenomenon that occurs when nuclear bang time is within the laser pulse<sup>12</sup>. Table I summarizes the characteristics of the typical backlighter used in these experiments.

The proton temporal diagnostic showed that the burn duration was  $\sim 150$  ps, and it determined the time at which the protons were emitted. The timing of the backlighter implosions was adjusted to provide radiographic images at different times relative to the onset of the laser-plasma interactions to be studied. This unique feature will be particularly important to future experiments with radiography of ICF implosions, allowing the study of capsule structure at any time; this contrasts with all nuclear ICF diagnostics used so far, which are based on self-emission and provide information about structure only at bang time. For example, hydrodynamic simulations have indicated that compression at the time of peak compression is a factor 2 larger than it is at bang time, but this has not yet been confirmed by direct nuclear measurement; proton radiography will allow us to investigate this by adjusting the timing of the backlighter.

**TABLE I. Summary of a typical proton backlighter**

<b>Capsule diameter</b>	420 $\mu\text{m}$
<b>Capsule wall thickness</b>	2.3 $\mu\text{m}$
<b>Fuel</b>	18 atm $D^3He$ gas
<b>Laser energy</b>	$\sim 10$ kJ
<b><math>T_e</math></b>	$\sim 12$ keV
<b>DD proton energy</b>	$\sim 3.5$ MeV
<b><math>D^3He</math> proton energy</b>	$\sim 15.3$ MeV
<b>DD proton yield</b>	$\sim 1 \times 10^9$
<b><math>D^3He</math> proton yield</b>	$\sim 2 \times 10^9$
<b>Bang time</b>	$\sim 450$ ps
<b>Burn duration</b>	$\sim 150$ ps
<b>Burn size (FWHM)</b>	$\sim 45 \mu\text{m}$



## B. The detection system

The detection system consists of a layered assembly of metallic foils and CR-39 detectors on which the projection radiography images were recorded<sup>9-11</sup>. CR-39 is a clear plastic whose chemical composition is  $C_{12}H_{18}O_7$ . When a charged particle passes through, it leaves a trail of damage along its track in the form of broken molecular chains and free radicals. The amount of local damage along the track is related to the local rate at which energy is lost by the particle. In particular, since  $dE/dx$  is different for protons at different energies, protons with different energies result in different track diameters.<sup>10,11</sup> In our experiments, two CR-39 detectors were sandwiched together with appropriately designed filters so that the front detector was sensitive to DD protons while the back one recorded only the  $D^3He$  protons (because the lower-energy protons were ranged out). Because this technique actually picked up each individual track (i.e. a nearly 100% efficiency), the CR-39 detector is uniquely suitable for experiments such as ours with relatively low proton flux.<sup>9</sup>

## C. Spatial resolution

Several possible sources of image broadening can compromise the fidelity of the radiography images, as illustrated in Fig. 3. Calculations and simulations have been

performed to estimate the effect of each. The characteristic image-broadening radii  $R_p$ ,  $R_{sc}$ , and  $R_d$  due to finite backlighter size, scattering at the subject, and broadening in the detector, respectively, can be written

$$R_p = \frac{A}{a + A} r_s \quad , \quad (3)$$

$$R_{sc} = \frac{aA}{a + A} \theta_{sc} \quad , \quad (4)$$

and

$$R_D = \frac{a}{a + A} r_D \quad . \quad (5)$$

Here  $r_s$  is the radius of the backlighter source,  $\theta_{sc}$  is the scattering angle at the subject,  $r_D$  is the radius for scattering in the detector,  $a$  is the source-subject distance, and  $A$  is the subject-detector distance. The source size  $r_s$  was described above and is typically 22.5  $\mu\text{m}$  (HWHM). Scattering in the subject was calculated using the Monte Carlo code TRIM<sup>21</sup>, which indicates a Gaussian distribution of angles with some 1/e radius  $\theta_{sc}$ , while scattering in the detectors and their filters results in a Gaussian lateral straggle with 1/e radius  $r_d$ . The net effect of these individual processes is convolution of image structure by the Gaussian  $\exp(-r^2/R_{tot}^2)$ , where

$$R_{tot} = \sqrt{R_p^2 + R_D^2 + R_{sc}^2} \quad . \quad (6)$$

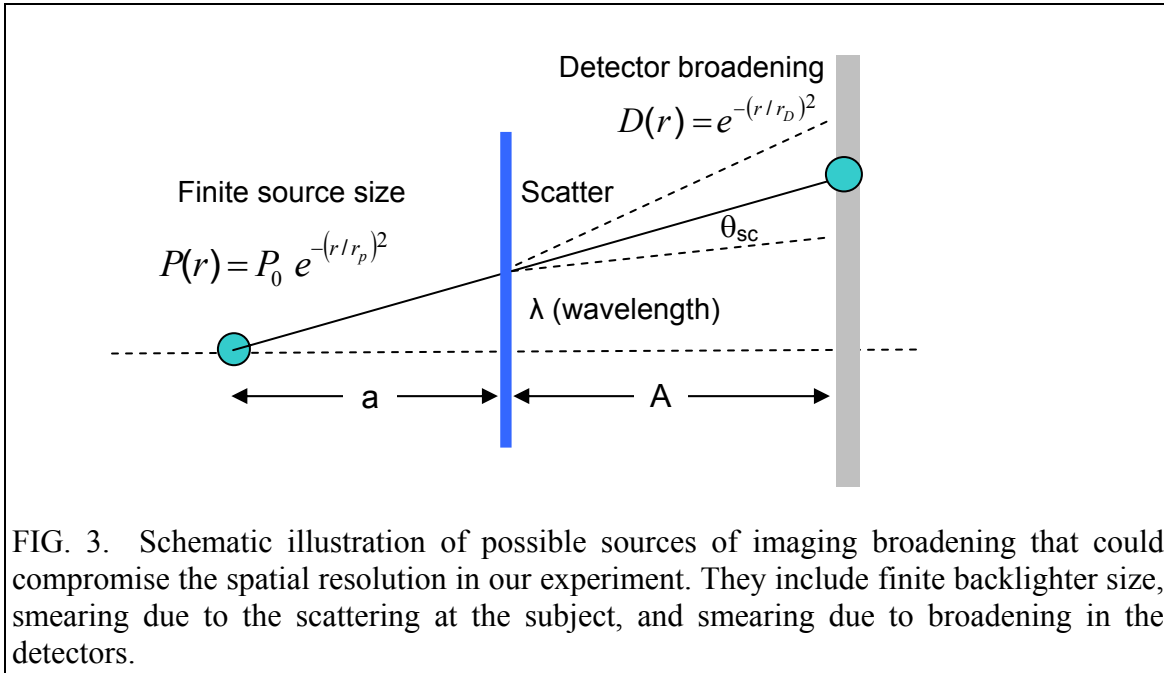


FIG. 3. Schematic illustration of possible sources of imaging broadening that could compromise the spatial resolution in our experiment. They include finite backlighter size, smearing due to the scattering at the subject, and smearing due to broadening in the detectors.

For structure with wavelength  $\lambda$  in the subject, the amplitude response in the image is the modulation transfer function which, for Gaussian smoothing with 1/e radius  $R_{tot}$ , is

$$MTF(\lambda) = e^{-(\pi R_{tot} / \lambda)^2} \quad . \quad (7)$$

If the minimum acceptable MTF is defined, this determines a minimum wavelength which contains two resolution elements with size  $\lambda_{\min}/2$ . If  $MTF_{\min} = 1/e$  the resolution limit is  $\pi R_{\text{tot}}/2$ , and if  $MTF_{\min} = 0.1$ , the limit is  $\sim R_{\text{tot}}$ .

### III. MEASURING E AND B FIELDS IN LASER-PRODUCED PLASMAS THROUGH 14.7-MeV PRPTON RADIOGRPHY

We have recently performed the first experiments on the OMEGA laser facility using monoenergetic protons for backlighting the E/B fields generated by a long-pulse, low-intensity laser interacting with plastic (CH) foils.<sup>9</sup> The setups of the experiments are illustrated in Figs. 4 and 5 for face-on and side-on radiography, respectively. The plasma and laser-plasma interactions, as well as the associated E/B fields, were induced by a single laser beam incident on a CH foil (henceforth called the *interaction beam*, which had wavelength  $0.351 \mu\text{m}$  and was incident  $23^\circ$  from the normal direction). The interaction beam delivered 500J or 250J in a  $800\mu\text{m}$  spot size during a 1-ns square pulse. No beam conditioning (phase plate or SSD) was applied to this beam. The resultant laser intensity was  $\sim 1 \times 10^{14} \text{ W/cm}^2$ .

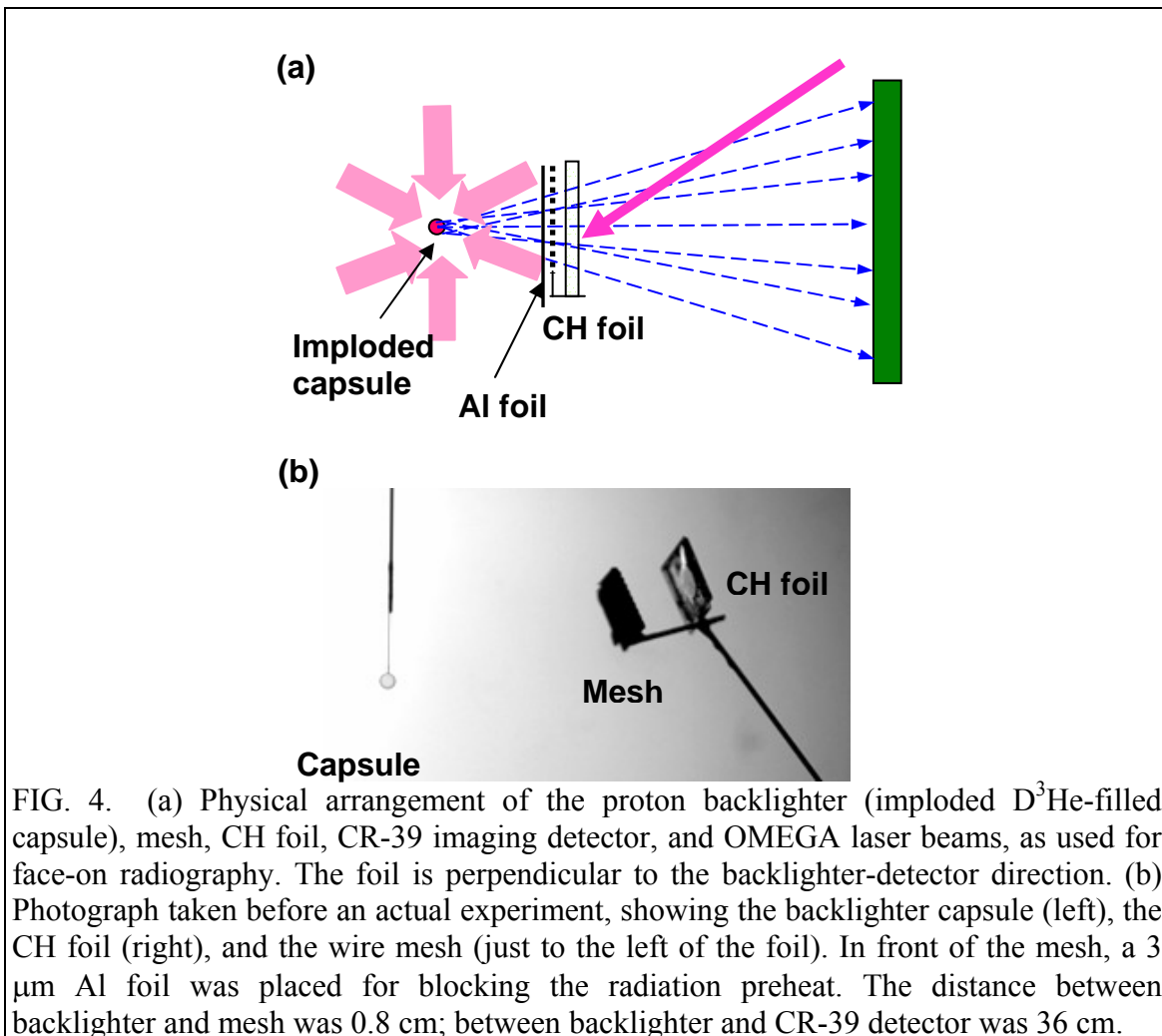


FIG. 4. (a) Physical arrangement of the proton backlighter (imploded  $\text{D}^3\text{He}$ -filled capsule), mesh, CH foil, CR-39 imaging detector, and OMEGA laser beams, as used for face-on radiography. The foil is perpendicular to the backlighter-detector direction. (b) Photograph taken before an actual experiment, showing the backlighter capsule (left), the CH foil (right), and the wire mesh (just to the left of the foil). In front of the mesh, a  $3 \mu\text{m}$  Al foil was placed for blocking the radiation preheat. The distance between backlighter and mesh was 0.8 cm; between backlighter and CR-39 detector was 36 cm.

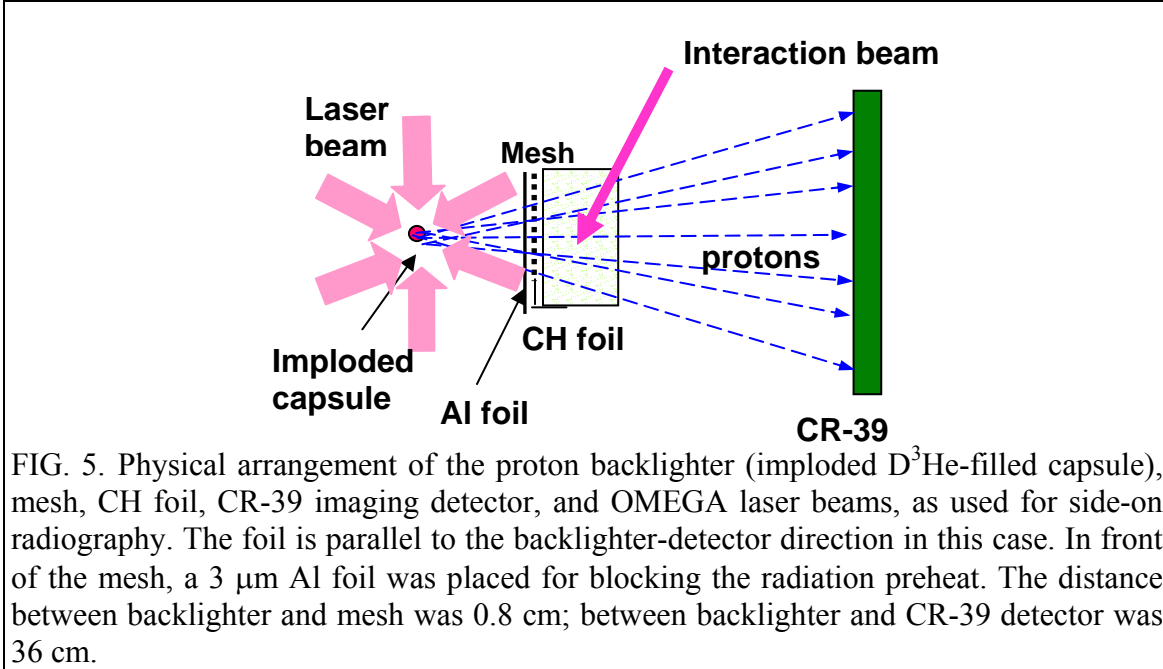


FIG. 5. Physical arrangement of the proton backlighter (imploded  $D^3He$ -filled capsule), mesh, CH foil, CR-39 imaging detector, and OMEGA laser beams, as used for side-on radiography. The foil is parallel to the backlighter-detector direction in this case. In front of the mesh, a 3  $\mu m$  Al foil was placed for blocking the radiation preheat. The distance between backlighter and mesh was 0.8 cm; between backlighter and CR-39 detector was 36 cm.

In each experiment, the protons passed through a wire mesh before impinging on the foil, and the distortion in the mesh pattern at the detector shows how the proton trajectories were deflected through interaction with the fields generated by laser-plasma interaction at the foil. The mesh was mounted on the foil assembly about 1 cm away<sup>9</sup>, and the center-to-center spacing of the mesh wires was either 150  $\mu m$  or 200  $\mu m$ . To prevent radiation from the imploded backlighter capsule (soft x rays, heat flux, visible light, etc) damaging the CH foil, or the wire mesh, a light-tight 3- $\mu m$  thick aluminum foil was attached to the mesh grid. The CR-39 detector was about 36 cm away. Since the burn duration of the  $D^3He$  implosion was short ( $\sim 150$  ps) relative to the duration of the foil illumination (1-ns), and since the relative timing of the implosion and the foil illumination was adjustable, it was possible to record images at different times relative to the foil illumination.

Under these experimental conditions, the principal mechanism for generation of magnetic fields results from plasma density and temperature gradients ( $\nabla T_e \times \nabla n_e$ ). Comprehensive LASNEX+LSP simulations<sup>8</sup> indicate that face-on radiography (with proton flux perpendicular to the surface of the foil (Fig. 5)) will be largely sensitive to the magnetic fields, while side-on radiography (with proton flux parallel to the foil surface (Fig 4)) will be sensitive to E fields. This allows E and B fields to be measured separately. The amount of deflection experienced by the two proton energies scales differently with the type of field that the protons pass through.

Sample face-on images recorded at different times are shown in Fig. 6. The images were acquired from six different shots; the laser timing was adjusted so the  $D^3He$  protons arrived at the foil at 0.0, 0.24, 0.3, 0.44, 0.65 and 0.87 ns, respectively, after the laser interaction beam was turned on. The diameter of the interaction beam at the foil was 800  $\mu m$ , and the pulse was 1 ns long with 500 J of energy. LASNEX calculations predict a hemispherical shell of peak magnetic field surrounding the ablative plasma bubble. The



magnitude of the magnetic field observed in the experiment can be estimated from the data by using the angular deflection of the proton beamlets from where they would be without the distortion, together with the geometry of the imaging system and the scale length for the plasma bubble in the direction perpendicular to the image. Preliminary estimates indicate that the B-field amplitude was  $\sim 0.5$  MG at  $t = 0.54$  ns.

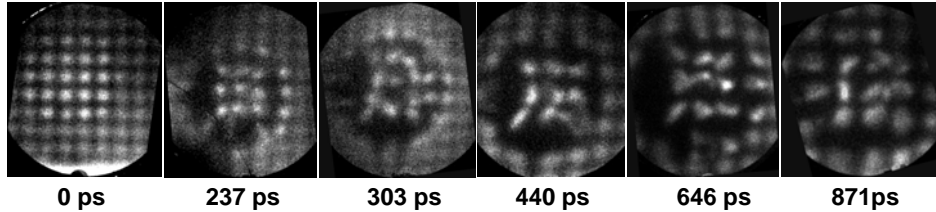


FIG. 6. Face-on images recorded on CR-39 detectors during different OMEGA shots. Each image is labeled by the difference between the time at which the 14.7-MeV  $D^3He$  protons passed the foil and the time when the foil was struck by the interaction laser beam. The first three images were made using a mesh with 150- $\mu m$  (center-to-center) spacing, while the last three were made with a 200- $\mu m$  mesh.

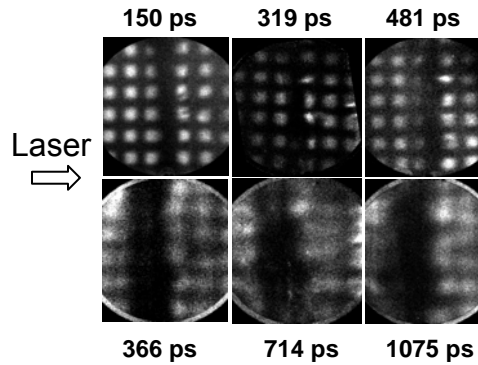


FIG. 7. Side-on images recorded on CR-39 detectors during three OMEGA shots. Each image is labeled by the difference between the time at which the protons passed the foil and the time when the foil was struck by a laser beam. The first-row are images taken with 14.7-MeV  $D^3He$  protons while second row were those from 3-MeV DD protons.

Side-on images recorded on the CR-39 detectors during three OMEGA shots are shown Fig. 7. Each image is labeled by the difference between the time at which the protons passed the foil and the time when the foil was struck by the interaction laser beam. The first-row are images taken with 14.7-MeV  $D^3He$  protons while the second row were those obtained from 3-MeV DD protons. Preliminary estimates indicate that the E-field amplitude was  $\sim 2 \times 10^8$  V/m.

#### IV. FUTURE WORK

With the recent and successful results of the 14.7-MeV-proton radiography experiments, summarized in Sec. III, we plan to extend this work in several fundamental ways.

## A. Expand the functionality of the monoenergetic backlighter sources

First, to expand the functionality of the backlighter sources, we will develop the capability of using two or three 14.7-MeV backlighters simultaneously. This will allow different views to be obtained on a single experiment, or, alternatively, different times over a several ns period. (Each monoenergetic source, the result of the nuclear burn of a D<sup>3</sup>He-filled exploding pusher, gates “on” for 150 ps.) In addition, we will develop particle backlighting with 9.5-MeV deuterons (D) from one branch (43%) of T<sup>3</sup>He reactions:

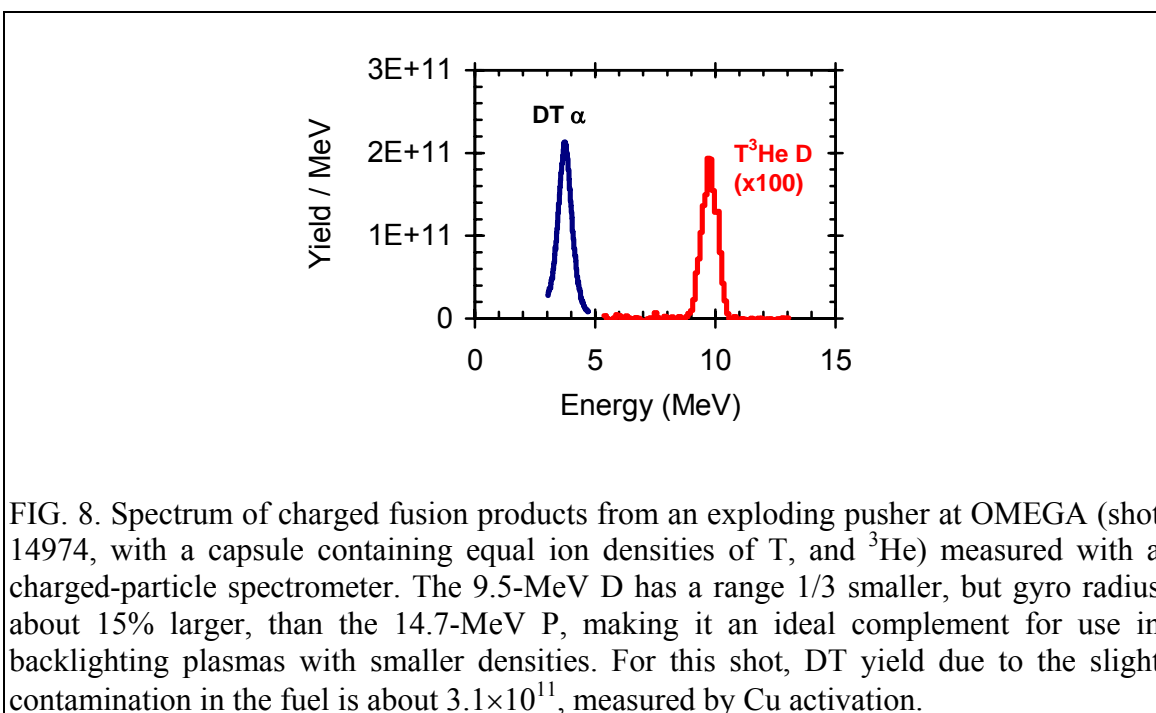


FIG. 8. Spectrum of charged fusion products from an exploding pusher at OMEGA (shot 14974, with a capsule containing equal ion densities of T, and <sup>3</sup>He) measured with a charged-particle spectrometer. The 9.5-MeV D has a range 1/3 smaller, but gyro radius about 15% larger, than the 14.7-MeV P, making it an ideal complement for use in backlighting plasmas with smaller densities. For this shot, DT yield due to the slight contamination in the fuel is about  $3.1 \times 10^{11}$ , measured by Cu activation.

Figure 8 shows both alphas and deuterons measured from a non-optimized, 60-beam OMEGA imploded-pusher implosion. With very different plasma stopping power and gyro radii, these two particles complement the 14.7-MeV proton by adding new information about both fields and areal density. In particular, the 9.5-MeV deuterons have a penetration and magnetic deflection that is distinctly different (and smaller) than the 14.7-MeV proton.

## B. Measuring the time evolution of E and B fields generated by laser-induced plasmas

The major physics objective of our program is to measure the evolution, over extended periods of time (0 to ~3 ns), of the B fields and the plasma plume originating from the single-laser foil interactions. The recent 14.7-MeV-proton backlighter data (Figs 6 and 7) sampled the magnetic fields in their early “expansion” phase only at 0.3 and 0.6 ns.<sup>8,9</sup> We plan to study the time evolution in smaller time steps and to later times.

Particular issues are: Will the region with fields continue to expand in a smooth fashion? At what time will the field strength begin to decay? Will the region with fields contract in size? And will chaotic structures begin to emerge at some point (as observed in the short-pulse interaction reported by Mackinnon)? 2-D LASNEX-LSP calculations<sup>8,9</sup> agree quite well with our data at 0.3 and 0.6 ns, but it is important to see whether simulations will continue to track the data out to much later times. Simulations predict substantial fields well after the interaction laser has turned off.<sup>8,9</sup>

### C. Radiographing implosions and their surrounding fields

Using the 14.7-MeV proton backlighter, we plan to radiograph the fields around spherically driven (and possibly asymmetrically driven) implosions. From the self-emission of 14.7-MeV  $D^3He$  protons, we learned that even spherically driven implosions can have substantial asymmetries in areal density, and also possess asymmetric external field structure<sup>14-19</sup>. Thus it would be important to examine, from more than one direction and at more than one time, using multiple backlighters, the field structure around the implosion. In addition, the energy losses of the 14.7-MeV backlighter protons that pass through the compressed capsule plasma would enable us to study radial density profiles.

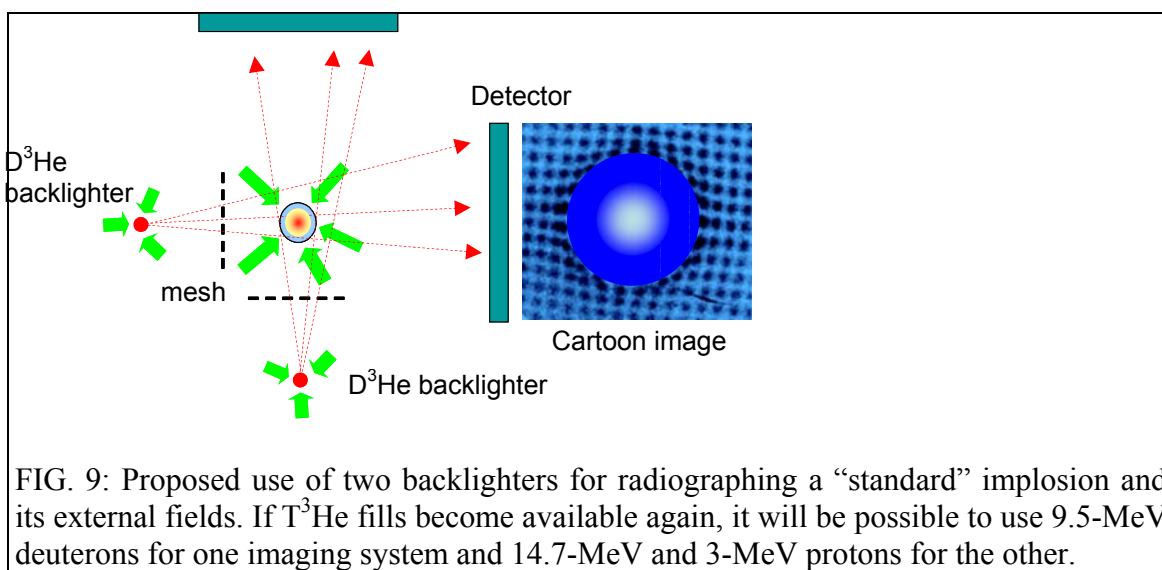


FIG. 9: Proposed use of two backlighters for radiographing a “standard” implosion and its external fields. If  $T^3He$  fills become available again, it will be possible to use 9.5-MeV deuterons for one imaging system and 14.7-MeV and 3-MeV protons for the other.

While the measurements of self-emitted 14.7-MeV  $D^3He$  protons give the integral  $\rho R = \int \rho dr$  along any radial path to a spectrometer (of which we have up to 10 on a single shot), they cannot determine the radial variation in  $\rho$  along that path. 2-D maps of energy loss vs. position in projection radiographs made with 14.7-MeV protons, together with appropriate inversion techniques, could provide that information; we will attempt to do this. Resolution is largely limited by the size of the burn region in the backlighter source (detector resolution is not a factor, since our CR-39 detectors have  $\sim 1 \mu m$  resolution<sup>11</sup>). The 3-MeV protons can be used to augment the 14.7-MeV information about fields outside the capsule in order to break possible degeneracy effects between E and B fields. A dual-backlighter experiment will be attempted (see Fig. 9) to provide a comprehensive mapping of fields and improved information about capsule density.

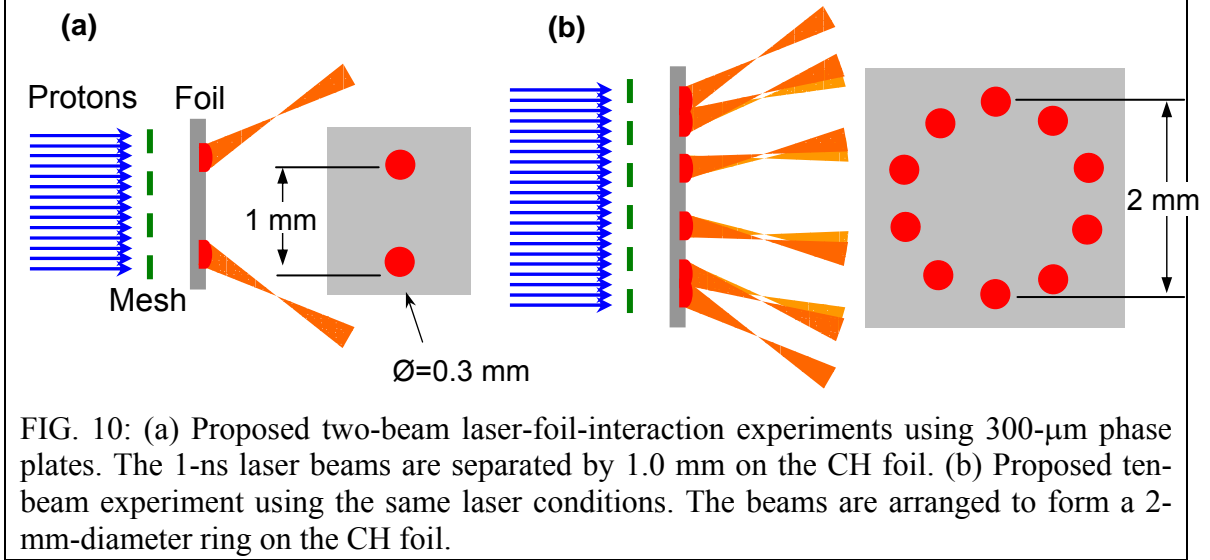


FIG. 10: (a) Proposed two-beam laser-foil-interaction experiments using 300- $\mu\text{m}$  phase plates. The 1-ns laser beams are separated by 1.0 mm on the CH foil. (b) Proposed ten-beam experiment using the same laser conditions. The beams are arranged to form a 2-mm-diameter ring on the CH foil.

#### D. Measuring the time evolution of fields generated by plasmas induced by multiple laser beams

The first object is to follow the evolution from early times ( $\leq 0.1$  ns), when two plasma plume/field structures are well separated [Fig. 10(a)], to later times (1- 3 ns) when the plumes and fields will have merged. We plan to study whether at intermediate times ( $\sim 1$  ns) chaotic structure might emerge as the plumes start to strongly interact, followed by a less chaotic, smoother decaying phase ( $\sim 2$  to 3 ns). As LASNEX+LSP can only simulate 2-D processes,<sup>8</sup> it will be interesting to see if a simple superposition of two single-spot simulations might match the observations, at least for a limited period. We will further investigate whether late in time ( $\geq 2$  ns), when the two laser-induced plasmas have merged, 2-D evolution might be “recovered”, and if the structure at that point is comparable in some sense to the late-time evolution data of the single-beam/foil experiments. We also propose to look at additional or longer times, or, as we conjecture is more important, to change the initial distance between the two laser spots and study the time evolution.

We also plan to irradiate a foil with a ring of 10 1-ns laser beams and follow the evolution of the interactions from early ( $\sim 0.2$  ns) to late ( $\sim 4$  ns) times [see Fig. 10(b)]. The ring diameter would be 2 mm, and each beam would use a 300- $\mu\text{m}$  (beam spot) phase plate. As the plasma structures grow and merge, they should approach a purely 2-D form that could be compared with LASNEX-LSP; it will be very important to see how well data and 2-D simulations agree. Such a comparison bears directly on the accuracy of 2-D simulations for modeling 10-beam, single-cone halfraum or hohlraum experiments (for which LASNEX is routinely used). In this context, it is worthwhile to point out that LASNEX has two magnetic field evolution packages, referred to as MAGF and HET, and, as recently reported by R. Town,<sup>8</sup> they lead to different predictions for the evolution of both the magnetic fields and  $T_e$  in hohlraum experiments (e.g. HET results in a higher  $T_e$ ).

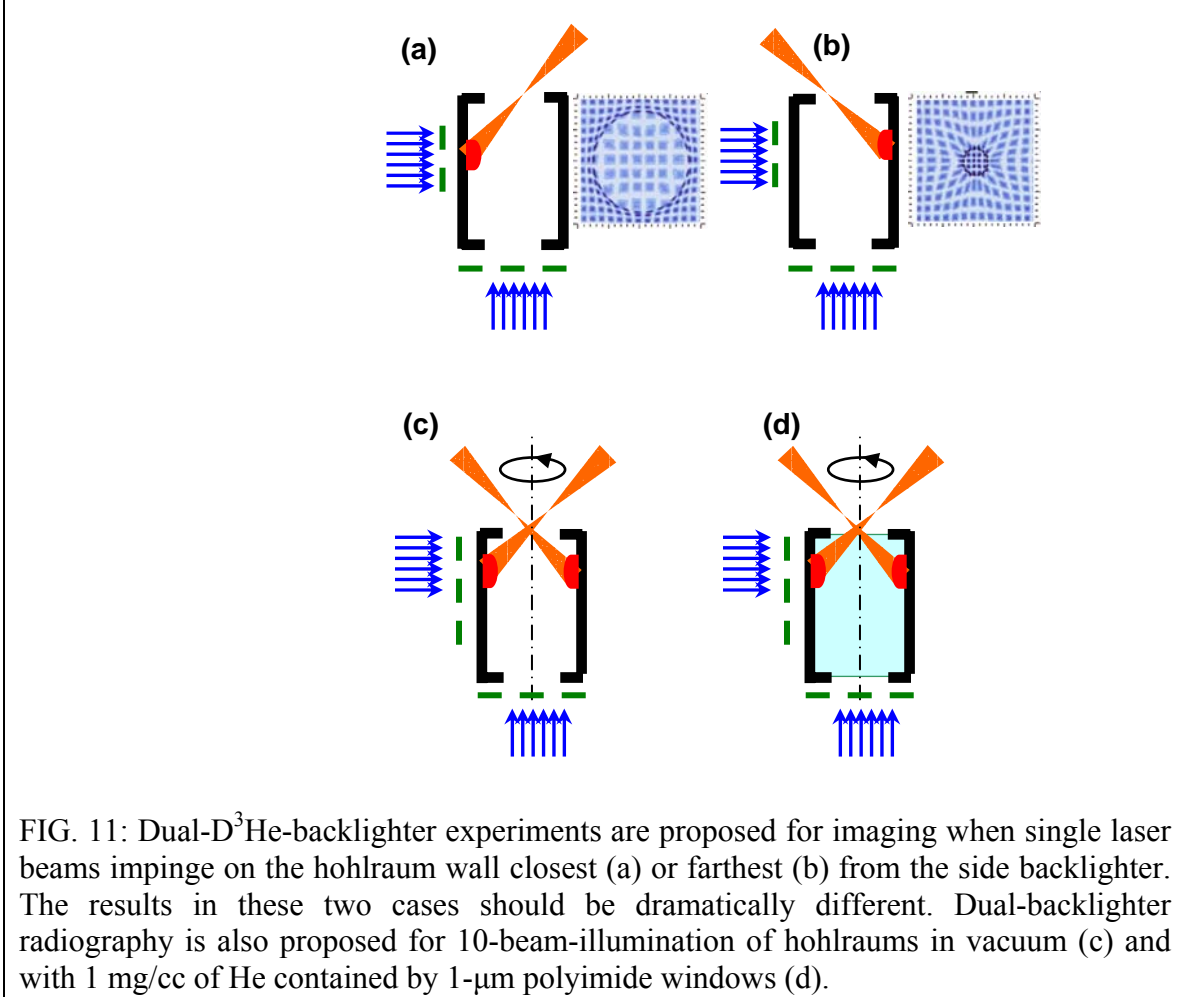


FIG. 11: Dual-D<sup>3</sup>He-backlighter experiments are proposed for imaging when single laser beams impinge on the hohlraum wall closest (a) or farthest (b) from the side backlighter. The results in these two cases should be dramatically different. Dual-backlighter radiography is also proposed for 10-beam-illumination of hohlraums in vacuum (c) and with 1 mg/cc of He contained by 1- $\mu$ m polyimide windows (d).

### E. Radiographing fields generated by laser-hohlraum interactions

To study laser-generated B fields in Au hohlraums, we are planning to conduct the following experiments: As illustrated in Fig. 11, a single beam would be shot at the side of a hohlraum closest to the backlighter [Fig. 11(a)] in one experiment, and then on the side farthest from the backlighter [Fig. 11(b)] in another experiment. Unlike all earlier experiments either performed or discussed, the configuration shown in Fig. 11(b) should result in “demagnified” images of the plasma region. For these experiments, dual 14.7-MeV P backlighters would be employed: one, as described above, from the side of the hohlraum, the other along the hohlraum axis.

Next, a Au hohlraum will be illuminated with 10 1-ns beams in a single cone, using 300- $\mu$ m phase plates. This would first be done in vacuum, and dual 14.7-MeV proton backlighters would simultaneously radiograph the fields from the side and from along the axis of the hohlraum [Fig. 11(c)]. To make this comparison even more NIF relevant, the previous experiment would be repeated but with 1 mg/cc of He gas in the hohlraum and with 1- $\mu$ m polyimide windows covering the LEH [Fig. 11(d)]. The results of this latter experiment should reflect the effects of the polyimide window – an increased  $T_e$  near the window through which the laser penetrated – and the tamping of Au blowoff

by the He. Dual backlighters would be used from the side and from along the axis of the hohlraum. These studies could give decisive data regarding the validity or limitations of the two LASNEX field-generating packages (MAGF and HET)<sup>8</sup>.

## **F. Studying astrophysical jets, magnetic compression experiments, and stopping power**

We will also explore different venues in which other workers might benefit from the use of the unique properties of the monoenergetic particle backlighters and their associated detector technology. Experiments for which measurements of fields and areal density would be important include laboratory astro-jet experiments, especially in the turbulent region around the head of the jet; on the basis of calculations that we've performed, such astro-lab experiments could, at the head of the jet, be sensitively probed for turbulently-generated fields using radiography with 14.7- and 3-MeV protons. In addition, areal density maps of the downstream plasma (and, as a calibration check, the cooler material upstream of the jet) could be accurately measured; this would help resolve perplexing uncertainties that now exist in these experiments.<sup>22</sup>

In a similar vein, magnetic-compression ICF experiments are being actively proposed.<sup>23</sup> One of the key issues is to measure, at peak convergence of the plasma cylinder, the areal density and especially the amplification of the B field ( $\sim 10^7$  G). Calculations we have done indicate that the amplified B field could readily be measured using 14.7-MeV-proton radiographs, with Lorentz deflections of the order of a few degrees. In addition, the areal density, estimated to be of order  $0.1 \text{ g/cm}^2$ , could also be easily determined through the energy loss of the 14.7-MeV protons (amounting to a few MeV).

Monoenergetic 14.7- and 3-MeV protons and 9.5-MeV deuterons would also be particularly useful for sensitively testing the accuracy of stopping power calculations<sup>24,25</sup>. Workers at LANL and MIT have suggested using such particles to investigate the predictions of different stopping models for well characterized plasmas, whether classical, degenerate, and/or strongly coupled.

## **V. CONCLUSION**

A novel monoenergetic proton backlighter source has been utilized at OMEGA to study electric (E) and magnetic (B) fields generated by laser-plasma interactions, and will be utilized in the future to radiograph OMEGA implosions. The backlighter consists of an imploding glass micro-balloon with  $\text{D}^3\text{He}$  fuel directly driven by 20 or fewer beams.  $\text{D}^3\text{He}$  reactions generate penetrating 14.7 MeV protons, and DD reactions generate 3.0 MeV protons. For quantitative study of E/B field structure, monoenergetic protons have several unique advantages compared to the broad energy spectrum used in previous experiments. In addition, the presence of two monoenergetic particles of very different energy is important for unraveling E and B field degeneracy. To this point, in recent experiments with a single laser beam (intensity  $\sim 10^{14} \text{ W/cm}^2$ ) interacting with a CH foil, B fields of  $\sim 0.5 \text{ MG}$  and E fields of  $\sim 2 \times 10^8 \text{ V/m}$  have been measured using proton

deflectometry. These results are consistent with LASNEX simulations of these experiments.

## ACKNOWLEDGMENTS

The work described here was performed in part at the LLE National Laser User's Facility (NLUF), and was supported in part by US DOE (Grant No. DE-FG03-03NA00058), LLNL (subcontract Grant No. B5543881), and LLE (subcontract Grant No. 412160-001G).

1. J. D. Lindl, *Inertial Confinement Fusion* (Springer-Verlag, New York, 1999).
2. S. Atzeni and J. Meyer-ter-Vehn, *The physics of Inertial Fusion* (Clarendon Oxford, 2004).
3. J. K. Kilkenney, S. G. Glendinning, S. G. Haan, *et al.*, Phys. Plasmas **1**, 1379 (1994).
4. B. A. Remington, S. V. Weber, M. M. Marinak, *et al.*, Phys. Rev. Lett. **73**, 545 (1994).
5. S. G. Glendinning, S. N. Dixit, B. A. Hammel, *et al.*, Phys. Rev. Lett. **78**, 3318 (1997).
6. A. J. Mackinnon, P. K. Patel, R. P. J. Town, *et al.*, Rev. Sci. Instrum. **75**, 3531 (2004).
7. L. Romagnani, J. Fuchs, M. Borghesi, *et al.*, Phys. Rev. Lett. **95**, 195001 (2005).
8. R. P. J. Town, W. E. Alley, M. J. Edwards, *et al.*, Bull. Am. Phys. Soc. **50**, 123 (2005).
9. C. K. Li, R. P. J. Town, F. H. Séguin *et al.*, submitted to Phys. Rev. Lett. (2006).
10. F. H. Séguin, J. A. Frenje, C. K. Li, *et al.*, Rev. Sci. Instrum. **74**, 975 (2003).
11. F. H. Séguin, J. D. DeCiantis, J. A. Frenje, *et al.*, Rev. Sci. Instrum. **75**, 3520 (2004).
12. C. K. Li, D. G. Hicks, F. H. Séguin, *et al.*, Phys. Plasmas **7**, 2578 (2000).
13. C. K. Li, F. H. Séguin, J. A. Frenje, *et al.*, Phys. Rev. Lett. **89**, 165002 (2002).
14. F. H. Séguin, C. K. Li, J. A. Frenje *et al.*, Phys. Plasmas **9**, 2725 (2002).
15. R. D. Petrasso, J. A. Frenje, C. K. Li, *et al.*, Phys. Rev. Lett. **90**, 095002 (2003).
16. J. A. Frenje, C. K. Li, F. H. Séguin, *et al.*, Phys. Plasmas **11**, 2480 (2004).
17. C. K. Li, F. H. Séguin, J. A. Frenje, *et al.*, Phys. Rev. Lett. **92**, 205001 (2004).
18. J. R. Rygg, J. A. Frenje, C. K. Li, *et al.*, accepted for publication in Phys. Plasmas (2006).
19. F. H. Séguin, J. D. DeCiantis, J. A. Frenje, *et al.*, accepted for publication in Phys. Plasmas (2006).
20. T. R. Boehly, D. L. Brown, R. S. Craxton, *et al.*, Opt. Commun. **133**, 495 (1997).
21. J. F. Ziegler and J. P. Biersack, *SRIM a code for calculations of the Stopping and Ranging of Ions in Matter*, Version 2003.26, 2004.
22. J. P. Knauer, private communications (2006).
23. R. Betti, private communication (2006).
24. C. K. Li and R. D. Petrasso, Phys. Rev. Lett. **70**, 3059 (1993).
25. N. Hoffman and C. Lee, Bull. Am. Phys. Soc. **46**, 106 (2001).